chemosensors

Article

Proline Enantiomers Discrimination by (L)-Prolinated Porphyrin Derivative Langmuir–Schaefer Films: Proof of Concept for Chiral Sensing Applications

Gabriele Giancane [1], Rosanna Pagano [2], Mario Luigi Naitana [3], Gabriele Magna [4], Manuela Stefanelli [4], Donato Monti [5], Roberto Paolesse [4], Simona Bettini [2,*] and Ludovico Valli [2]

1 Department of Cultural Heritage, Università del Salento, Via D. Birago, 48, I-73100 Lecce, Italy
2 Department of Biological and Environmental Sciences and Technologies, DISTEBA, University of Salento, Via per Arnesano, I-73100 Lecce, Italy
3 Department of Science, Roma Tre University, Viale Guglielmo Marconi 446, I-00146 Rome, Italy
4 Department of Chemical Science and Technologies, University of Rome Tor Vergata, Via della Ricerca Scientifica 1, I-00133 Rome, Italy
5 Department of Chemistry, Sapienza University of Rome, Piazzale Aldo Moro 5, I-00185 Rome, Italy
* Correspondence: simona.bettini@unisalento.it; Tel.: +39-0832299445

Abstract: A porphyrin derivative functionalized with the L-enantiomer of proline amino acid was characterized at the air–pure water interface of the Langmuir trough. The porphyrin derivative was dissolved in dichloromethane solution, spread at the air–subphase interface and investigated by acquiring the surface pressure vs. area per molecule Langmuir curves. It is worth observing that the behavior of the molecules of the porphyrin derivative floating film was substantially influenced by the presence of L-proline amino acid dissolved in the subphase (10^{-5} M); on the contrary, the physical chemical features of the floating molecules were only slightly influenced by the D-proline dissolved in the subphase. Such an interesting chirality-driven selection was preserved when the floating film was transferred onto solid supports by means of the Langmuir–Schaefer method, but it did not emerge when a spin-coating technique was used for the layering of the tetrapyrrolic derivatives. The obtained results represent proof of concept for the realization of active molecular layers for chiral discrimination: porphyrin derivatives, due to their intriguing spectroscopic and supramolecular properties, can be functionalized with the chiral molecule that should be detected. Moreover, the results emphasize the crucial role of the deposition technique on the features of the sensing layers.

Keywords: porphyrins; proline; Langmuir–Schaefer techniques; chirality; supramolecular aggregation; chiral discrimination

Citation: Giancane, G.; Pagano, R.; Naitana, M.L.; Magna, G.; Stefanelli, M.; Monti, D.; Paolesse, R.; Bettini, S.; Valli, L. Proline Enantiomers Discrimination by (L)-Prolinated Porphyrin Derivative Langmuir–Schaefer Films: Proof of Concept for Chiral Sensing Applications. *Chemosensors* **2022**, *10*, 331. https://doi.org/10.3390/chemosensors10080331

Academic Editor: Nicole Jaffrezic-Renault

Received: 19 July 2022
Accepted: 12 August 2022
Published: 13 August 2022

1. Introduction

Porphyrins are tetrapyrrolic macrocycles, typically thought of as molecular building blocks with unique physical–chemical properties suitable for several applications [1–5], including the design of thin organic layers for sensing devices [6–8]. The high extinction coefficient, the wide π-conjugation, the emission properties, the photochemical stability, the modulation of their characteristics by introducing a peripheral substituent or changing the central metal ion and the possibility of tuning their aggregation state upon π-π stacking are among the main features that make porphyrins so interesting in this research field [9]. Further, these compounds can be engineered and regulated as molecular Legos in supramolecular networks [10,11] conferring indispensable and superior features for detection systems development based on electrochemical, optical and gravimetric transduction modes [12,13]. In this context, porphyrins integration within thin layers has been reported through several self-assembly approaches, including Langmuir–Blodgett (LB) techniques, the Langmuir–Schaefer (LS) approach, drop casting, spin coating, and layer by layer [14–16]. LB and LS, above all, are self-assembly humid deposition techniques, known

to guarantee high control of the deposition parameters and high reproducibility of the induced molecular organization from the air–aqueous subphase interface towards the solid support [17,18]. Such an induced molecular organization and aggregation/configuration were reported to be fundamental for analytes recognition, making deposition through the LB or LS approach essential to ensure sensor functioning [19]. Moreover, this approach has been also used for the assembly of organized porphyrin-based materials expressing chirality at a supramolecular level [20–22] and allowing enantiodiscrimination [23]. The development of stereoselective sensing devices is particularly urgent for environmental and health safety [24,25]. Indeed, the chirality of wastes (pesticides, hormones, pharmaceuticals, amino acids) needs to be considered, especially for the unpredictable effects of the interaction between diverse enantiomers and biological ecosystems [26–29]. Stereoselective platforms are also intriguing in the early disease diagnosis field. Within this framework, a chiral free-base porphyrin derivative bearing L-proline functionality on a meso phenyl position named H_2PL(-) (Scheme 1) was selected, and the obtained LS films have been tested for the fluorescent detection of L-proline. H_2PL(-) is a very interesting molecule due to its reported tendency to aggregate in hydroalcoholic medium at micromolar concentration, providing chiral porphyrin assemblies through a hydrophobic effect [30]. In similar aggregative conditions, the corresponding Zn derivative provides chiral suprastructures via a two-step mechanism driven by the Zn–carboxylate coordination in the second, slower, stage [30]. Nonetheless, the chirality transfer for these systems to the solid state is not obvious, and still remains a challenge. For example, optically active films on glass slides have been achieved by drop casting a toluene solution of Zn prolinated complex, whose chiroptical features were found to be strictly dependent on the solvent used, as well as glass roughness [31]. Alternatively, a chiral film based on the same derivatives was obtained when layered onto ZnO nanoparticles' surface, and was able to discriminate limonene enantiomers in nanogravimetric gas sensing measurements [32].

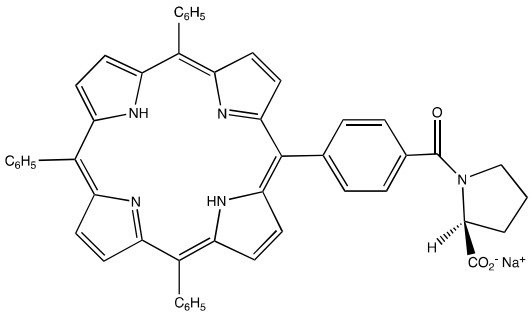

H_2PL(-)

Scheme 1. Molecular structure of the chiral porphyrin H_2PL(-) used in these studies.

L-proline was chosen as the model analyte, since it coincides with the chiral peripheral substituent, which plays a key role in derivatives stereospecific aggregation thanks to carboxylate–inner nitrogen atoms interaction [30]. L-proline, indeed, is an essential cyclic amino acid with fundamental physiological roles as a precursor of collagen, salivary proteins, antimicrobial peptides, cornifins (proteins of the cell envelope) and also of plant cell wall proteins [33]. Balancing and monitoring the L-proline amount is fundamental [34], since this amino acid can induce beneficial tissue regeneration, but can also be related to tumor disease progression [35]. Further, L-proline accumulation was confirmed to be a marker of plant cell stress [36].

The aim of this work is to spectroscopically investigate how L-proline and D-proline could modify the aggregation state of the chiral porphyrin derivative in order to find a thin layer selective for the anticlockwise form of the amino acid. Thus, in this contribution, the Langmuir trough was utilized for the deep characterization of the tetrapyrrolic derivative behavior at the air/water subphase interface and at the air/aqueous subphase contain-

ing L- and D-proline, respectively. Upon transferring L-porphyrin derivative by means of the LS approach onto solid supports, the tendency to further aggregate L-porphyrin derivative within thin film was monitored as quenching of the fluorescent emission, and this was employed to develop a proof of concept of a fluorescent sensing platform in the 10^{-4}–10^{-8} M L-proline concentration range. Interestingly, the film deposited through the spin-coating approach did not show any ability to detect the amino acid, underlining the fundamental role of the aggregation state and the molecular organization induced by the LS approach. Moreover, the LS film of L-proline is not spectroscopically influenced by the flux of D-proline, confirming the possibility of selectively sensing the L-proline enantiomer.

The obtained results are very promising for the design of a molecularly active layer of porphyrin derivatives, ensuring enantiodiscrimination by changing the peripheral substituent as in the described proof of concept.

2. Materials and Methods

H_2PL(-) was synthetized according to the procedure reported in [30] and dissolved in dichloromethane at 10^{-4} M concentration for the Langmuir experiments. L-proline and D-proline were purchased from Merck and used as received. Amino acids concentration for the subphase preparation in the Langmuir experiments was 10^{-5} M.

Porphyrin derivative dichloromethane solution was spread on the aqueous subphase by means of a gas-tight syringe. A NIMA trough, thermostated at 293 K, was used to obtain the Langmuir films and the surface pressure variation was recorded by a platinum Wilhelmy plate immersed through the film–subphase interface. After dichloromethane evaporation, the two Teflon barriers of the Langmuir trough were symmetrically moved at a constant speed of 5 cm^2 min^{-1}. An aliquot of 120 μL of dichloromethane solution of the porphyrin derivate was spread at the air/subphase interface for each experiment. After solvent evaporation and upon floating molecules compression at the subphase surface, the monolayer undergoes phase changes, as in the case of the three-dimensional gases, liquids and solids. These phase changes can be monitored by the surface pressure Π as a function of the area occupied by the floating film, thus sketching a curve called isotherm. In the so-called "gaseous" phase, the molecules are too distant, and they weakly interact; the Π values indeed are very low. In the liquid state, generally called the expanded monolayer phase, the molecules are randomly arranged and Π values start to increase with a slope variation in the curve. When the area occupied by the molecules is progressively and slowly reduced, the condensed phase appears. In the condensed phase, molecules are closely stacked and oriented; the area per molecule is similar to the cross-section area of the monolayer molecule, and this value corresponds to the limit surface area. The obtained surface layer was transferred by the Langmuir–Schaefer (LS) deposition technique; that is, the horizontal variant of the traditional Langmuir–Blodgett (LB) technique. The LB method is carried out by simply reiterating withdrawal and immersion cycles of a substrate through the monolayer. The vertical transfer, typical of LB films, may be unsuccessful when considerably rigid monolayers are formed at the air–water interface. In such cases, it is also possible to use the LS method. The substrate, previously hydrophobized, is horizontally lowered in order to graze the hydrophobic terminations of the floating molecules. When the substrate is detached from the water surface, transfer onto the support takes place, preserving the same molecular orientation. Using this method, the floating monolayer will be subject to less destructive forces and molecular rearrangement than would occur when using the classic LB method. UV-Visible spectra of the thin solid films were recorded by means of a Cary 5000 (Varian). Fluorescence emission was recorded by a Horiba Fluorolog equipped with a stage for solid samples.

Spin-coated films were obtained from porphyrin derivative solution in dichloromethane with a concentration of 10^{-3} M at a spin rate of 3200 rpm [14].

For the fluorescent sensing experiments, L-proline and D-proline solutions were fluxed on the slide quartz placed in ad hoc shaped Teflon cell by means of a peristaltic pump at 1 mL min^{-1}.

3. Results and Discussion

3.1. Langmuir Films Characterization and H_2PL(-) Film Deposition

Floating films of H_2PL(-) spread from a dichloromethane solution were characterized at the air–pure water interface of a Langmuir trough by recording the isotherm curves surface pressure vs. area per molecule [23] (Figure 1a). The isotherm curve shows the typical profile of hydrophobic porphyrins spread on water subphase. A rapid change in the curve slope is observed at about 150 Å^2 molecule^{-1}, and a limit area of 120 Å^2 molecule^{-1} is recorded. It can be deduced that the molecules are stacked in an aggregate floating film under the action of the moving barriers of the Langmuir trough [37].

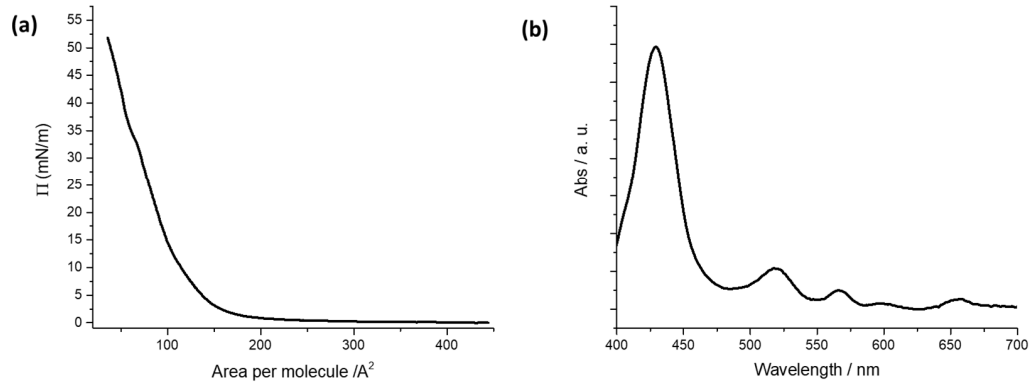

Figure 1. (**a**) Surface pressure vs. area per molecule curve for the porphyrin derivative dissolved in dichloromethane (10^{-4} M) and spread at the air–ultrapure water interface. (**b**) Absorption spectrum of LS films of H_2PL(-) deposited from pure water.

H_2PL(-) floating film was transferred from the air/water subphase interface using the horizontal variation of the LB method [38]; that is, the LS technique. The LS technique ensures high reproducibility of the physical chemical characteristics of the transferred film, a uniform covering of the solid substrate, and it is possible to control and to preserve the floating film features during the transfer process [39–41].

A surface pressure deposition value was chosen from Langmuir isotherm curves of the floating film. The deposition process was performed at a surface pressure value corresponding to the steepest branch of the isotherm curve [42]. So, five LS runs of H_2PL(-) were transferred at 22 mN m^{-1} on quartz slides and the UV-visible spectrum of the transferred film was recorded (see Figure 1b). The Soret band of the solid LS film was centered at 428 nm, and the four Q-bands were located at 519, 564, 597 and 654 nm.

3.2. Physical Chemical Study of L- and D-Proline Interaction with H_2PL(-) Langmuir and Langmuir Schaefer Films

In order to evaluate the possible interactions among H_2PL(-) with the two enantiomers of proline, the Langmuir curves [23] of the H_2PL(-) floating layer were recorded dissolving L- and D-proline in the aqueous subphase. In detail, the isotherm curves of the derivative spread from dichloromethane solution were recorded on: (i) pure water subphase, (ii) subphase containing L-proline water solution (10^{-5} M) and (iii) subphase containing D-proline water solution (10^{-5} M). The surface pressure vs. area per molecule curves recorded for the three different systems appear to be very different (Figure 2). In particular, the presence of L-proline in the aqueous subphase clearly influenced the isotherm curve profile of H_2PL(-) (orange line in Figure 2). A very long pseudo-gaseous phase was present, with an abrupt slope change at 180 Å^2 molecule^{-1}, typical of highly aggregated floating molecules [37]. The limiting area per molecule was about 160 Å^2 molecule^{-1}, suggesting an interaction among the molecules spread onto the subphase and the L-proline dissolved in water. D-proline dissolved in the subphase induced a shift in the Langmuir curves towards smaller area per molecule (gray line), even though the isotherm profile and the limiting area per molecule did not significantly change compared to the effect of L-proline. These

preliminary results suggest that both the proline enantiomers interacted with the floating molecules, even if L-proline induced a strong change in the curve profile.

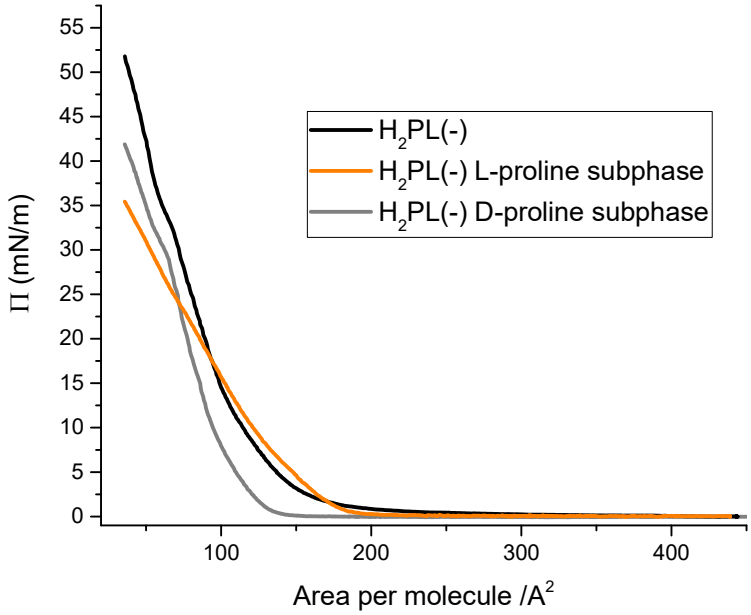

Figure 2. Surface pressure vs. area per molecule curves for porphyrin derivative dissolved in dichloromethane (10^{-4} M) and spread at the air–aqueous interface in presence of 10^{-5} M L-proline (orange line) and D-proline (gray line).

The possibility of preserving the ability of H_2PL(-) to change its supramolecular aggregation, mainly in the presence of L-proline, was explored using the LS technique [38] and by means of the well-known spin-coating thin-film transfer method [43]. A comparison of these two deposition techniques was performed in order to evaluate the different role of the self-aggregation process that takes place in the floating molecules upon the effect of the barriers' slow movement [44,45], and the solvent evaporation driven by the centrifugal force that promotes the film formation in the spin-coating method [14]. The Langmuir films of the porphyrin derivative were transferred by means of the LS approach on solid supports after spreading on pure water and L- and D-proline containing subphases. Surface pressure deposition values were chosen from Langmuir isotherm curves of the floating film. The deposition process was performed at surface pressure value corresponding to the steepest branch of isotherm curve [42]. So, five LS runs of H_2PL(-) were transferred at 22 mN m^{-1} on quartz slides, in the case of molecules spread on aqueous subphase containing D-proline at a concentration of 10^{-5} M and, as reported in Section 3.1, from ultrapure water subphase. In the case of H_2PL(-) spread on L-proline containing subphase, the deposition process was performed at 18 mN m^{-1}.

In the sake of clarity, the UV-visible spectrum of H_2PL(-) diluted dichloromethane solution is reported in Figure 3a (red line), whilst the spectrum of both spin coated and LS film of H_2PL(-) transferred from ultrapure water is reported in Figure 3b (purple dotted line and black line, respectively). The Soret band for the solution spectrum is located at 418 nm, and this is in agreement with a preferential monomeric conformation [30]; instead, the two deposition approaches induce a different organization within the film: the Soret band is centered at 422 nm for the spin-coated film and 428 nm for the LS film, suggesting the influence of the deposition method on the supramolecular arrangement of the layered molecules.

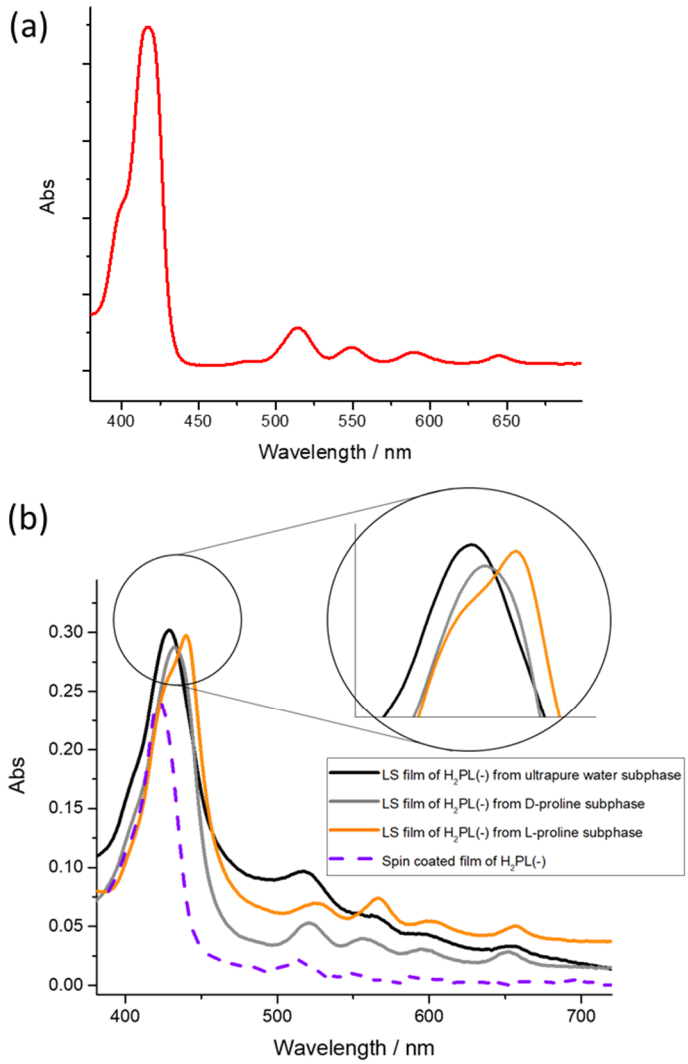

Figure 3. Absorption spectra of (**a**) dichloromethane solution of H_2PL(-) and (**b**) LS films of H_2PL(-) transferred from pure water subphase, D-proline and L-proline containing subphase (black, gray and orange spectra, respectively). A magnification of the Soret band in the three different situations is reported in the inset. Dotted line represents the UV-visible spectrum of H_2PL(-) transferred by spin-coating method.

When L-proline was dissolved in the subphase and the H_2PL(-) floating film was transferred, the Soret band was redshifted about 15 nm in comparison with the one obtained from pure water subphase, and it was located at 442 nm. Further, the Soret band of the monomeric form of H_2PL(-) appears as a pronounced shoulder at about 424 nm (Figure 3b, orange line). Thus, it can be concluded that the presence of L-proline in the subphase favors further aggregation of the spread H_2PL(-) molecules. Concerning the LS film of H_2PL(-), from the containing D-proline subphase, a slight redshift of about 3 nm of the Soret band, compared with the porphyrin film obtained from ultrapure water subphase (Figure 3b, gray line), was recorded, confirming that the porphyrin derivative preferentially interacts with the L-enantiomer of the proline.

It can be supposed that the aggregation mechanism for H_2PL(-) molecules within the LS film is driven by weak interactions, mainly hydrogen bonds, among peripheral proline substituent carboxylate groups and inner nitrogen atoms [31]. Proline amino acid in the subphase affected this process, favoring further aggregation, according to the recorded redshift of about 15 nm of the Soret band. The formation of J-type aggregates has already

been reported in the literature for similar systems [30]. The preferential interaction of the floating layer with L-proline should be ascribed to the chirality of the substituent.

3.3. Preliminary Sensing Tests

Evidence that the aggregation/disaggregation process is driven by the chiral recognition between the peripheral substituent and the L-form of the amino acid dissolved in the subphase prompted us to evaluate the effect of L- and D-proline aqueous solution fluxed on LS film of H_2PL(-) deposited from air–pure water interface. In particular, five layers of H_2PL(-) were deposited on hydrophobized quartz substrates. Furthermore, in order to evaluate the role of the deposition technique on the sensitivity of the porphyrin derivative layers towards proline, the response of H_2PL(-) spin-coated film to both the enantiomers of proline was tested. L- and D-proline water solution at a concentration of 10^{-4} M were fluxed, by means of a peristaltic pump, both on the LS and on spin-coated films.

From the spectra reported in Figure 4a, it is evident that both the L-proline and D-proline fluxes do not influence the absorption profile of the H_2PL(-) spin-coated film. On the contrary, a redshift of 5 nm of the Soret band was observed for the H_2PL(-) LS film, and an evident shoulder appeared at 445 nm after the L-proline flux; instead, the effect of the flux of D-proline was not detectable (Figure 4b). According to the data recorded on the LS film of H_2PL(-) from pure water and L-proline containing subphase, it is suggested that the deposition process promotes the transfer of H_2PL(-) in monomeric form and that L-proline, both in subphase or fluxed in water solution, induces the aggregation of the H_2PL(-) molecules.

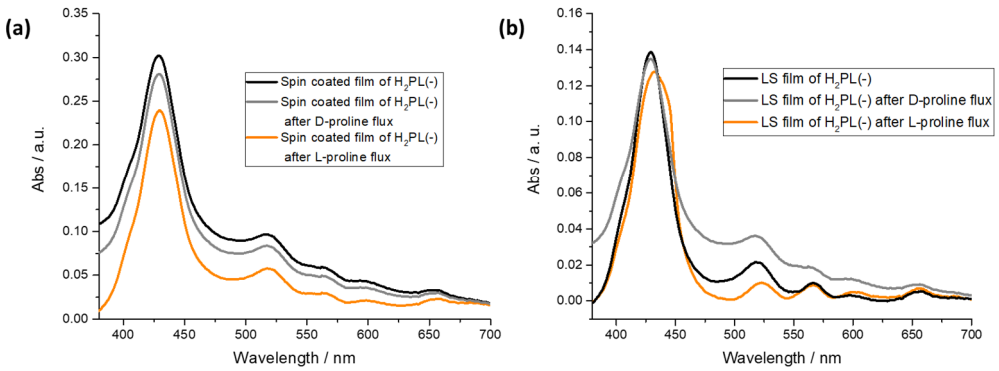

Figure 4. Effect of D- and L-proline flux on H_2PL(-) spin-coated film (**a**) and H_2PL(-) LS film from water subphase (**b**).

As a proof of concept of the chiral-sensing device for L-proline in liquid phase, the fluorescence spectroscopy was used as transduction method [14]. The emission spectrum of the LS film (five layers) of H_2PL(-) was monitored as a function of the concentration of L-proline and D-proline aqueous solution in the range 10^{-8} M–10^{-4} M. Fluorescence emission of porphyrin derivatives is, in fact, particularly sensible to aggregation phenomena [46–48], as well as charge and/or energy transfer among the active molecules and the analyte [49,50]. The D-proline water flux did not promote evident variation of the emission intensity (λ_{exc} = 430 nm, Figure 5a). On the other side, as reported in Figure 5b, an evident quenching of fluorescence intensity of the LS film of H_2PL(-) (λ_{exc} = 430 nm) was observed when L-proline was fluxed on the thin film. The further molecular aggregation induced by the L-proline, as demonstrated by means of visible absorption spectroscopy, promoted a self-quenching phenomenon [51], reducing the emission intensity.

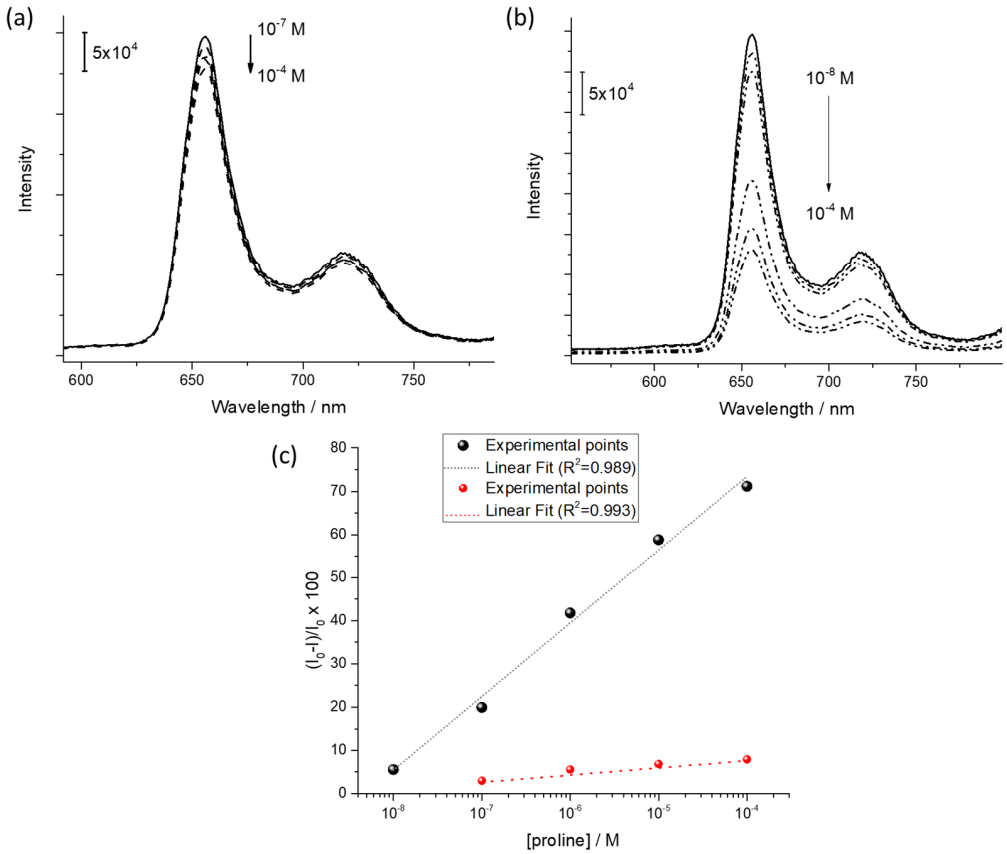

Figure 5. Quenching induced by (**a**) D-proline flux and (**b**) L-proline flux on fluorescence emission of H_2PL(-) LS film. (**c**) Logarithmic relation between the fluorescence quenching and the L-proline (black dots) and D-proline (red dots) concentration.

Further, in the considered range, a linear relationship in a semilogarithmic scale was used to monitor the fluorescence quenching as a function of the L-proline and D-proline concentration (black and red dots, respectively, in Figure 5c).

This represents a very intriguing starting point for the design of amino acid enantioselective porphyrin-based sensors. The design and synthesis of porphyrin derivatives ad hoc functionalized with chiral amino acid could be used as an efficient platform for chiral discrimination.

4. Conclusions

A free-base porphyrin derivative bearing, on its periphery, the L-enantiomer of proline has been used in order to prepare films via two different approaches: the first one—the Langmuir–Schaefer technique—is suitable for the development of weak interactions and supramolecular structures, and the second—the spin-coating method—generally brings out less organized structures. The first procedure provides evidence that the floating layer of the porphyrin molecules carrying L-proline selectively interfaces with L-proline dissolved in the subphase; conversely, the D-derivative slightly affects the aggregation state of the porphyrin floating film. It is remarkably that this fascinating chirality-inspired phenomenon has been kept alive when the corresponding LS multilayers have been deposited. On the other hand, such typical and systematic behavior could not be retained when spin-coated films have been prepared. Summing up these investigations, we have obtained further confirmation about the ability of the LS method to shield and preserve supramolecular organization and physical–chemical characteristics, even in the solid state as thin films.

Finally, promising exploratory measurements concerning the chiral discriminating ability of the deposited LS multilayers have been successfully obtained. Investigations

on the behavior at the air–water interface and the sensing capability towards proline enantiomers of the chiral free-base porphyrin derivative bearing D-proline functionality on a meso phenyl position are being carried out, and the results will be presented in future work. Eventually, it will be very interesting to characterize the chiral features of the deposited films in order to fully understand the physical–chemical nature of the discrimination process.

Author Contributions: Conceptualization, G.G., M.S. and S.B.; Synthesis of porphyrin, D.M., M.S.; Air/water interface measurements, G.G.; Film deposition, R.P. (Rosanna Pagano) and S.B.; Sensing measurements and rationalization, S.B., D.M., G.M., M.L.N.; Writing, R.P. (Rosanna Pagano); Supervision, L.V. and R.P. (Roberto Paolesse); Funding Acquisition, L.V. and R.P. (Roberto Paolesse). All authors have read and agreed to the published version of the manuscript.

Funding: This research was funded by the European Innovation Council through the INITIO-FET Project (Grant Agreement: 828779).

Institutional Review Board Statement: Not applicable.

Informed Consent Statement: Not applicable.

Acknowledgments: This research was supported by the PRIN 2017 (protocol number 2017PBXPN4_003) and by "Research for Innovation" POR PUGLIA FESR-FSE 2014/2020 Ricerca Regione Puglia.

Conflicts of Interest: The authors declare no conflict of interest.

References

1. Vittorino, E.; Giancane, G.; Bettini, S.; Valli, L.; Sortino, S. Bichromophoric Multilayer Films for the Light-Controlled Generation of Nitric Oxide and Singlet Oxygen. *J. Mater. Chem.* **2009**, *19*, 8253–8258. [CrossRef]
2. Kou, J.; Dou, D.; Yang, L. Porphyrin Photosensitizers in Photodynamic Therapy and Its Applications. *Oncotarget* **2017**, *8*, 81591–81603. [CrossRef]
3. Kingsbury, C.J.; Senge, M.O. The Shape of Porphyrins. *Coord. Chem. Rev.* **2021**, *431*, 213760. [CrossRef]
4. Singh, G.; Chandra, S. Unravelling the Structural-property Relations of Porphyrinoids with Respect to Photo- and Electro-chemical Activities. *Electrochem. Sci. Adv.* **2021**, e2100149. [CrossRef]
5. Chen, Y.; Li, A.; Huang, Z.-H.; Wang, L.-N.; Kang, F. Porphyrin-Based Nanostructures for Photocatalytic Applications. *Nanomaterials* **2016**, *6*, 51. [CrossRef] [PubMed]
6. Lvova, L.; Di Natale, C.; Paolesse, R. Porphyrin-Based Chemical Sensors and Multisensor Arrays Operating in the Liquid Phase. *Sens. Actuators B Chem.* **2013**, *179*, 21–31. [CrossRef]
7. Ishihara, S.; Labuta, J.; Van Rossom, W.; Ishikawa, D.; Minami, K.; Hill, J.P.; Ariga, K. Porphyrin-Based Sensor Nanoarchitectonics in Diverse Physical Detection Modes. *Phys. Chem. Chem. Phys.* **2014**, *16*, 9713–9746. [CrossRef] [PubMed]
8. Qi, Z.-L.; Cheng, Y.-H.; Xu, Z.; Chen, M.-L. Recent Advances in Porphyrin-Based Materials for Metal Ions Detection. *Int. J. Mol. Sci.* **2020**, *21*, 5839. [CrossRef]
9. Paolesse, R.; Nardis, S.; Monti, D.; Stefanelli, M.; Di Natale, C. Porphyrinoids for Chemical Sensor Applications. *Chem. Rev.* **2017**, *117*, 2517–2583. [CrossRef] [PubMed]
10. Zhang, L.; Wang, T.; Jiang, J.; Liu, M. Chiral Porphyrin Assemblies. *Aggregate* **2022**, e198. [CrossRef]
11. Van der Weegen, R.; Teunissen, A.J.P.; Meijer, E.W. Directing the Self-Assembly Behaviour of Porphyrin-Based Supramolecular Systems. *Chem. Eur. J.* **2017**, *23*, 3773–3783. [CrossRef]
12. Negut, C.; Van Staden, R.-I.S.; Van Staden, J.F.V. Porphyrins-as Active Materials in the Design of Sensors. An Overview. *ECS J. Solid State Sci. Technol.* **2020**, *9*, 51005. [CrossRef]
13. Porphyrin-Based Nanostructures for Sensing Applications. Available online: https://www.hindawi.com/journals/js/2009/856053/ (accessed on 2 May 2022).
14. Buccolieri, A.; Hasan, M.; Bettini, S.; Bonfrate, V.; Salvatore, L.; Santino, A.; Borovkov, V.; Giancane, G. Ethane-Bridged Bisporphyrin Conformational Changes As an Effective Analytical Tool for Nonenzymatic Detection of Urea in the Physiological Range. *Anal. Chem.* **2018**, *90*, 6952–6958. [CrossRef]
15. Nishiyama, F.; Yokoyama, T.; Kamikado, T.; Yokoyama, S.; Mashiko, S. Layer-by-Layer Growth of Porphyrin Supramolecular Thin Films. *Appl. Phys. Lett.* **2006**, *88*, 253113. [CrossRef]
16. Al-Alwani, A.J.; Mironyuk, V.N.; Pozharov, M.V.; Gavrikov, M.V.; Glukhovskoy, E.G. Formation and Phase Behavior of Porphyrin/Arachidic Acid Mixed Systems and Morphology Study of Langmuir-Schaefer Thin Films. *Soft Mater.* **2022**, *20*, 310–321. [CrossRef]
17. Arnold, D.P.; Manno, D.; Micocci, G.; Serra, A.; Tepore, A.; Valli, L. Gas-Sensing Properties of Porphyrin Dimer Langmuir–Blodgett Films. *Thin Solid Film.* **1998**, *327–329*, 341–344. [CrossRef]

18. Giancane, G.; Bettini, S.; Valli, L.; Bracamonte, V.; Carraro, M.; Bonchio, M.; Prato, M. Supramolecular Organic–Inorganic Domains Integrating Fullerene-Based Acceptors with Polyoxometalate-Bis-Pyrene Tweezers for Organic Photovoltaic Applications. *J. Mater. Chem. C* **2021**, *9*, 16290–16297. [CrossRef]
19. Manera, M.G.; Ferreiro-Vila, E.; García-Martín, J.M.; Cebollada, A.; García-Martín, A.; Giancane, G.; Valli, L.; Rella, R. Enhanced Magneto-Optical SPR Platform for Amine Sensing Based on Zn Porphyrin Dimers. *Sens. Actuators B Chem.* **2013**, *182*, 232–238. [CrossRef]
20. Wang, T.; Liu, M. Langmuir–Schaefer Films of a Set of Achiral Amphiphilic Porphyrins: Aggregation and Supramolecular Chirality. *Soft Matter* **2008**, *4*, 775–783. [CrossRef]
21. Lin, L.; Wang, T.; Lu, Z.; Liu, M.; Guo, Y. In Situ Measurement of the Supramolecular Chirality in the Langmuir Monolayers of Achiral Porphyrins at the Air/Aqueous Interface by Second Harmonic Generation Linear Dichroism. *J. Phys. Chem. C* **2014**, *118*, 6726–6733. [CrossRef]
22. Colozza, N.; Stefanelli, M.; Venanzi, M.; Paolesse, R.; Monti, D. Fabrication of Langmuir–Blodgett Chiral Films from Cationic (L)-Proline-Porphyrin Derivatives. In *Porphyrin Science by Women*; World Scientific: Singapore, 2021; pp. 878–884, ISBN 9789811223549.
23. Bettini, S.; Grover, N.; Ottolini, M.; Mattern, C.; Valli, L.; Senge, M.O.; Giancane, G. Enantioselective Discrimination of Histidine by Means of an Achiral Cubane-Bridged Bis-Porphyrin. *Langmuir* **2021**, *37*, 13882–13889. [CrossRef]
24. Randazzo, R.; Gaeta, M.; Gangemi, C.; Fragalà, M.; Purrello, R.; D'Urso, A. Chiral Recognition of L- and D- Amino Acid by Porphyrin Supramolecular Aggregates. *Molecules* **2018**, *24*, 84. [CrossRef]
25. Yu, F.; Chen, Y.; Jiang, H.; Wang, X. Recent Advances of BINOL-Based Sensors for Enantioselective Fluorescence Recognition. *Analyst* **2020**, *145*, 6769–6812. [CrossRef]
26. Ye, J.; Zhao, M.; Niu, L.; Liu, W. Enantioselective Environmental Toxicology of Chiral Pesticides. *Chem. Res. Toxicol.* **2015**, *28*, 325–338. [CrossRef]
27. Wang, P.; Zhang, Q.; Li, Y.; Zhu, C.; Chen, Z.; Zheng, S.; Sun, H.; Liang, Y.; Jiang, G. Occurrence of Chiral Organochlorine Compounds in the Environmental Matrices from King George Island and Ardley Island, West Antarctica. *Sci. Rep.* **2015**, *5*, 13913. [CrossRef]
28. Ternes, T.A. Occurrence of Drugs in German Sewage Treatment Plants and Rivers1Dedicated to Professor Dr. Klaus Haberer on the Occasion of His 70th Birthday.1. *Water Res.* **1998**, *32*, 3245–3260. [CrossRef]
29. González-González, R.B.; Sharma, P.; Singh, S.P.; Américo-Pinheiro, J.H.P.; Parra-Saldívar, R.; Bilal, M.; Iqbal, H.M.N. Persistence, Environmental Hazards, and Mitigation of Pharmaceutically Active Residual Contaminants from Water Matrices. *Sci. Total Environ.* **2022**, *821*, 153329. [CrossRef]
30. Monti, D.; De Rossi, M.; Sorrenti, A.; Laguzzi, G.; Gatto, E.; Stefanelli, M.; Venanzi, M.; Luvidi, L.; Mancini, G.; Paolesse, R. Supramolecular Chirality in Solvent-Promoted Aggregation of Amphiphilic Porphyrin Derivatives: Kinetic Studies and Comparison between Solution Behavior and Solid-State Morphology by AFM Topography. *Chem. Eur. J.* **2010**, *16*, 860–870. [CrossRef]
31. Stefanelli, M.; Savioli, M.; Zurlo, F.; Magna, G.; Belviso, S.; Marsico, G.; Superchi, S.; Venanzi, M.; Di Natale, C.; Paolesse, R.; et al. Porphyrins Through the Looking Glass: Spectroscopic and Mechanistic Insights in Supramolecular Chirogenesis of New Self-Assembled Porphyrin Derivatives. *Front. Chem.* **2020**, *8*, 587842. [CrossRef]
32. Stefanelli, M.; Magna, G.; Zurlo, F.; Caso, F.M.; Di Bartolomeo, E.; Antonaroli, S.; Venanzi, M.; Paolesse, R.; Di Natale, C.; Monti, D. Chiral Selectivity of Porphyrin–ZnO Nanoparticle Conjugates. *ACS Appl. Mater. Interfaces* **2019**, *11*, 12077–12087. [CrossRef]
33. Patriarca, E.J.; Cermola, F.; D'Aniello, C.; Fico, A.; Guardiola, O.; De Cesare, D.; Minchiotti, G. The Multifaceted Roles of Proline in Cell Behavior. *Front. Cell. Dev. Biol.* **2021**, *9*, 2236. [CrossRef]
34. Zeußel, L.; Aziz, C.; Schober, A.; Singh, S. PH-Dependent Selective Colorimetric Detection of Proline and Hydroxyproline with Meldrum's Acid-Furfural Conjugate. *Chemosensors* **2021**, *9*, 343. [CrossRef]
35. D'Aniello, C.; Patriarca, E.J.; Phang, J.M.; Minchiotti, G. Proline Metabolism in Tumor Growth and Metastatic Progression. *Front. Oncol.* **2020**, *10*, 776. [CrossRef]
36. Forlani, G.; Funck, D. A Specific and Sensitive Enzymatic Assay for the Quantitation of L-Proline. *Front. Plant. Sci.* **2020**, *11*, 582026. [CrossRef]
37. Petty, M.C. *Langmuir-Blodgett Films: An Introduction*; Cambridge University Press: Cambridge, UK, 1996; ISBN 978-0-511-62251-9.
38. Rella, R.; Siciliano, P.; Quaranta, F.; Primo, T.; Valli, L.; Schenetti, L.; Mucci, A.; Iarossi, D. Gas Sensing Measurements and Analysis of the Optical Properties of Poly [3-(Butylthio)Thiophene] Langmuir–Blodgett Films. *Sens. Actuators B Chem.* **2000**, *68*, 203–209. [CrossRef]
39. Guo, P.; Zhang, L.; Liu, M. A Supramolecular Chiroptical Switch Exclusively from an Achiral Amphiphile. *Adv. Mater.* **2006**, *18*, 177–180. [CrossRef]
40. Zhang, Y.; Chen, P.; Liu, M. A General Method for Constructing Optically Active Supramolecular Assemblies from Intrinsically Achiral Water-Insoluble Free-Base Porphyrins. *Chem. Eur. J.* **2008**, *14*, 1793–1803. [CrossRef]
41. Urtizberea, A.; Natividad, E.; Alonso, P.J.; Andrés, M.A.; Gascón, I.; Goldmann, M.; Roubeau, O. A Porphyrin Spin Qubit and Its 2D Framework Nanosheets. *Adv. Funct. Mater.* **2018**, *28*, 1801695. [CrossRef]
42. Ulman, A. Part Two-Langmuir–Blodgett Films. In *An Introduction to Ultrathin Organic Films*; Ulman, A., Ed.; Academic Press: Cambridge, MA, USA, 1991; pp. 101–236, ISBN 978-0-08-092631-5.

43. Ingrosso, C.; Curri, M.L.; Fini, P.; Giancane, G.; Agostiano, A.; Valli, L. Functionalized Copper(II)−Phthalocyanine in Solution and As Thin Film: Photochemical and Morphological Characterization toward Applications. *Langmuir* **2009**, *25*, 10305–10313. [CrossRef]
44. Bliznyuk, V.N.; Assender, H.E.; Briggs, G.A.D. Surface Glass Transition Temperature of Amorphous Polymers. A New Insight with SFM. *Macromolecules* **2002**, *35*, 6613–6622. [CrossRef]
45. Peltonen, J.P.K.; He, P.; Rosenholm, J.B. Influence of UV Irradiation on Unsaturated Fatty Acid Monolayers and Multilayer Films: X-Ray Diffraction and Atomic Force Microscopy Study. *Langmuir* **1993**, *9*, 2363–2369. [CrossRef]
46. Maiti, N.C.; Mazumdar, S.; Periasamy, N. J- and H-Aggregates of Porphyrin−Surfactant Complexes: Time-Resolved Fluorescence and Other Spectroscopic Studies. *J. Phys. Chem. B* **1998**, *102*, 1528–1538. [CrossRef]
47. Ohno, O.; Kaizu, Y.; Kobayashi, H. J-aggregate Formation of a Water-soluble Porphyrin in Acidic Aqueous Media. *J. Chem. Phys.* **1993**, *99*, 4128–4139. [CrossRef]
48. Lang, K.; Mosinger, J.; Wagnerová, D.M. Photophysical Properties of Porphyrinoid Sensitizers Non-Covalently Bound to Host Molecules; Models for Photodynamic Therapy. *Coord. Chem. Rev.* **2004**, *248*, 321–350. [CrossRef]
49. Concepcion, J.J.; House, R.L.; Papanikolas, J.M.; Meyer, T.J. Chemical Approaches to Artificial Photosynthesis. *Proc. Natl. Acad. Sci. USA* **2012**, *109*, 15560–15564. [CrossRef]
50. Urbani, M.; Grätzel, M.; Nazeeruddin, M.K.; Torres, T. Meso-Substituted Porphyrins for Dye-Sensitized Solar Cells. *Chem. Rev.* **2014**, *114*, 12330–12396. [CrossRef]
51. Ghosh, M.; Nath, S.; Hajra, A.; Sinha, S. Fluorescence Self-Quenching of Tetraphenylporphyrin in Liquid Medium. *J. Lumin.* **2013**, *141*, 87–92. [CrossRef]